



# ELECTROCHEMICAL ASSESSMENT OF CONCRETE TERNARY INHIBITORS USED IN RETARDING CORROSION OF STEEL REINFORCEMENT

Abdulrahman, A. S<sup>1</sup>. and Mohammad Ismail<sup>2</sup>

<sup>1</sup>Department of Mechanical Engineering, Federal University of Technology, PMB 65, Minna, Nigeria

<sup>2</sup>Construction Research Centre, Universiti Teknologi Malaysia, 81310 UTM, Johor Bahru, Johor, Malaysia

E-Mail: [asipita.salawu@futminna.edu.ng](mailto:asipita.salawu@futminna.edu.ng)

## ABSTRACT

Corrosion of steel reinforcement in concrete is generally considered as an electrochemical process which reduces the service life of a structure exposed to chloride ions attack. Therefore, laboratory experiments were performed in order to ascertain the effectiveness and sustainability of ternary inhibitors (calcium nitrite, ethanolamine and eco-friendly green *Bambusa Arundinacea*) in protecting steel reinforcement in concrete from corrosion attack due to chloride. Concrete mix was designed to be 30MPa with 0.45 and 0.65 W/C ratios. Inhibitors additions were 2% and 4% by weight of cement. The specimens were subjected to various durability corrosion test (using; electrochemical impedance spectroscopy (EIS)) for 360 days. The results showed that *Bambusa arundinacea* has exhibited lowest corrosion rate, highest concrete resistance and highest polarization resistance ( $R_p$ ) values for the period of exposure, compared to calcium nitrite and ethanolamine. *Bambusa arundinacea* may be considered a better substitute for nitrite and amine- based corrosion inhibiting admixtures for durable concrete structures due to its viability, versatility and eco-friendliness.

**Keywords:** steel reinforcement, concrete, corrosion, green Inhibitor, sustainability, EIS.

## 1. INTRODUCTION

Deterioration and collapse of reinforced concrete structures is due to corrosion and a major problem in the construction industry especially in the coastal region, which are characterized by high salinity. The cost of repairing or replacing deteriorated structures has become a major liability to government and the private sectors. The primary cause of this deterioration is the corrosion of steel reinforcement due to chlorides whose main source is the seawater and deicing salts (Abdulrahman *et al.*, 2012; Jing and Wu, 2011; Królikowski and Kuziak, 2011; Ismail *et al.*, 2010a).

In many countries with rapidly developing infrastructures, economies in construction have led to poor quality concrete and low concrete cover to the steel resulting in corrosion problems. Also, the developed economies are not left out of this endemic problem, according to Indrajit *et al.* (2011), who reported that one out of nine of existing concrete bridges in United States of America is deficient as a result of chloride ions from deicing salts on highway bridges exposed to freeze-thaw and dry-wet cyclic which translated to 31.7% of the nation's 73, 800 structurally deficient bridges and this alone consumes 3.1% of their GDP.

Therefore, the major daunting challenge facing the civil engineering community is to execute projects in tandem with nature using the concept of sustainable development involving the uses of environmental benign materials produced at a reasonable cost. In the context of concrete, which is the predominant building material, it is imperative to identify corrosion inhibitor which is eco-friendly to salvage the life span of concrete structure exposed to harsh environments.

Several solutions to this problem have been proposed and tested, albeit to date no ideal solution has

been found workable (Abdulrahman *et al.*, 2011a; Boltryk *et al.*, 2011; Rwamamara and Simonson, 2012). Thus, the principle of the corrosion inhibitor admixture is to prevent the chloride ions from reacting with the steel surface and also to increase the time needed for the chloride ions to penetrate through the concrete cover. Corrosion inhibitors are chemical substance which decreases the corrosion rate when present in the corrosion system at a suitable concentration without significantly changing the concentration of any other corrosive agent (Ismail *et al.*, 2010b).

In recent studies (Abdulrahman *et al.*, 2011b; Raja and Sethuraman, 2008; Uhlig, 2004) green inhibitors have proved more effective and environmentally benign than organic and inorganic inhibitors in chemical and petrochemical industries. Consequently, more work in this area is necessary in order to ascertain the compatibility and suitability of green inhibitor to reinforced concrete to minimize the risk posed by organic and inorganic inhibitors to environmental and sustainability.

## 2. EXPERIMENTAL PROCEDURE

### 2.1. Materials used

Ordinary Portland Cement (OPC) was used in this research. The chloride was admixed into the concrete as magnesium chloride of analytical reagent grade. The concentrations of Magnesium chloride used was 1.5% and 4.5% by mass of cement and the corresponding chloride concentrations were 0.94% and 2.82% respectively. Coarse aggregates of size 20 mm and 10 mm of quartzite origin were used in the ratio of 1.78:1 to satisfy the overall grading requirement of coarse aggregate (Ismail *et al.*, 2011).



Land quarried sand passing through ASTM sieve no. (4.57mm) conforming to zone II classification of British standard was used as fine aggregate. The sand has a fineness modulus of 2.5. Tap water was used for the preparation of specimens. All the concrete mixes were designed for similar workability with slump of 30-60 mm. The water content was kept constant to 230 kg/m<sup>3</sup> for the desired slump in all the mixes to have similar workability. The water-cement ratio (w/c) used were 0.45 and 0.65. The fresh density of concrete was then obtained as per guidelines specified by British method of mix selection (DOE) to be 2380Kg/m<sup>3</sup>. The design mix is as presented in companion paper (Abdulrahman *et al.*, 2012).

## 2.2. Corrosion rate measurement

Corrosion behaviours of embedded steel in concrete were monitored by electrochemical impedance spectroscopy (EIS) and linear polarization resistance (LPR) using the Shikoku Research Institute Portable Rebar Corrosion Meter (SRI-CM-III). Measurements were done at the corrosion potential; the amplitude of the sine wave perturbation was 10mV in frequency range of 10 KHz to 10 mHz, 25 points sweep density per frequency decade were collected. Standard silver chloride electrode was used as reference, stainless steel disc as central and guard counter electrode and 16 mm diameter mild steel was used as working electrode. EIS measurements were carried out after 360 days of exposure to wet and dry cycles. Initially the specimens were cured in seawater for 28 days at a laboratory temperature of 28°C after 24h of casting. Polarization resistance ( $R_p$ ) (that is, charge transfer resistance) values obtained from Nyquist plot which was calculated from the diameter of the semi-circle extrapolated in the low frequency range between 10 KHz and 10 mHz. By assuming B as 26 mV, the corrosion current density ( $I_{corr}$ ) ( $\mu$  A/cm<sup>2</sup>) was calculated using Stern-Geary equation in accordance with earlier work of Vishnudevan, Thangavel (2006).

$$I_{corr} = \frac{B}{R_p}$$

Where B is a constant which is a function of the anodic and cathodic Tafel slopes,  $b_a$  and  $b_c$

$$B = \frac{b_a \times b_c}{2.303(b_a + b_c)}$$

$$Z(\omega) = R_c + R_p / ((1 + \omega^2 [R_p^2 C_{dl}^2]) - (j\omega C_{dl} R_p^2) / ((1 + \omega^2 [R_p^2 C_{dl}^2]))$$

Where  $\omega$  = angular frequency of the applied signal,  $C_{dl}$  = double layer capacitance.

From the above equation, the value of  $Z(\omega)$  at very low frequencies becomes

$$Z \omega \rightarrow 0(\omega) = R_c + R_p$$

In this investigation B value of 26 mV was used for both active and passive state of rebar, since the system was premixed with magnesium chloride except control sample (Vishnudevan, Thangavel, 2006).

Corrosion rate (mmpy) of the exposed rebar is measured by using following formula:

$$\text{Corrosion rate (mm/year)} = \frac{0.00327 \times a \times I_{corr}}{n \times D}$$

Where  $I_{corr}$  = corrosion current density in  $\mu$  A/cm<sup>2</sup>,  $a$  = atomic weight of iron, that is, 55.845 g/mol,  $n$  = no. of electrons exchanged in corrosion reaction, that is 2 for iron,  $D$  = density of steel (7.85 g/cm<sup>3</sup>). The double layer capacitance was calculated from  $R_p$  values using the formula:

$$C_{dl} = \frac{1}{2\pi \times F_{max} \times R_p}$$

Where  $F_{max}$  = frequency maximum,  $R_p$  = polarization resistance.

For calculation of the corrosion current density for EIS, the assumed model for the steel/concrete interface is shown in Figure-1. Steel-concrete interface is represented by a simple equivalent electric circuit. The equivalent circuit consists of concrete resistance  $R_c$  in series with the interface impedance. The interface impedance consists of polarization resistance  $R_p$  in parallel with a double layer capacitance  $C_{dl}$ . Frequency dependent impedance  $Z(\omega)$  of the electrical equivalent circuit shown in Figure-1 is given by the following expression:

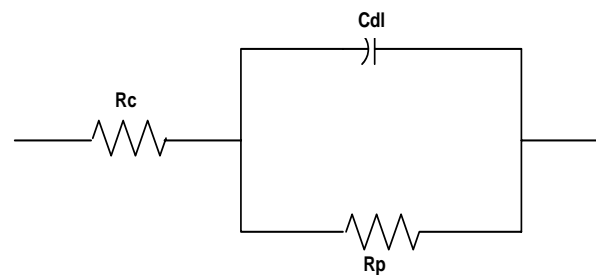


Figure-1. Equivalent electric circuit for steel/concrete interface.

And at very high frequencies

$$Z \omega \rightarrow \infty(\omega) = R_c$$

Therefore  $R_c$  measured at high frequency can be subtracted from  $R_p + R_c$  measured at low frequency to give a compensated value of  $R_p$  free of ohmic interferences in high resistivity medium like concrete.



Impedance behaviour of an electrode may be expressed in Nyquist plots of  $Z''(\omega)$  (imaginary component) as a function of  $Z'(\omega)$  (real component). The Nyquist plot would show a semicircle with frequency increasing in a counterclockwise direction. At very high frequency, the imaginary component  $Z''(\omega)$  disappears, leaving only the concrete resistance,  $R_c$ . At very low frequency,  $Z''(\omega)$  again disappears leaving a sum of  $R_c$  and  $R_p$ . Thus the radius of the semi circle is  $R_p/2$ .

### 3. RESULTS AND DISCUSSIONS

#### 3.1. Corrosion potential ( $E_{corr}$ ) of embedded steel

Corrosion potential ( $E_{corr}$ ) monitoring and electrochemical impedance spectroscopy (EIS) was the techniques used for this study. These techniques have been extensively used in laboratory investigations of the corrosion behaviour of reinforced concrete exposed to chloride-containing environment (Ann *et al.*, 2006; De-Schutter and Luo, 2004; Kondratova *et al.*, 2003). EIS has the major advantage of providing the possibility of establishing a physical interpretation of the processes involved.

Figures 2-3 shows the typical corrosion potential ( $E_{corr}$ ) behaviour, as a function of exposure time in days, of reinforced concrete with w/c ratio of 0.45 subjected to wet and dry cycle. Starting potential was 10 mV vs. Ag/AgCl electrode. Starting at approximately six months of exposure, potentials of reinforcing steel were not indicative of corrosion likelihood in the concrete mix according to ASTM C876-09.

Generally, going by the potential results of all the inhibitors, their inhibitions were adequate for 0.45 w/c ratios. But Bambusa arundinacea stand out for excellent inhibition for both mixes as can be seen in Figures 2-3. However, with increasing periods of exposure, the potential values tended to decrease (become more positive). This is due to the hydration process of cement paste which corresponds to the compressive strength values recorded. This work demonstrates that adequate good protection is already provided with 2% of inhibitor that is below the recommended amount (4%) (Pech-Canul and Castro, 2002).

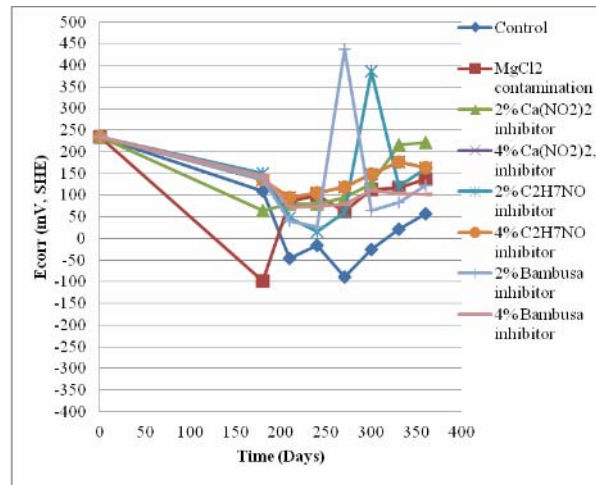


Figure-2. Corrosion potential as a function of exposure time for a 0.45 w/c with 1.5%  $MgCl_2$  addition.

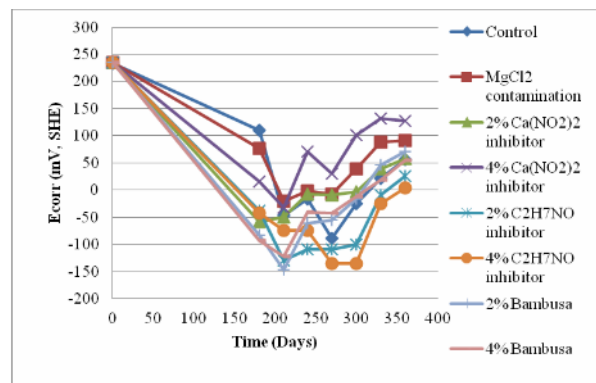


Figure-3. Corrosion potential as a function of exposure time for a 0.45 w/c with 4.5%  $MgCl_2$  addition.

#### 3.2 Corrosion current

Corrosion current density ( $I_{corr}$ ) represents instantaneous rate of corrosion at the particular time of voltage measurement, and changes frequently over time for specimen according to Raafat *et al.* (2011).  $I_{corr}$  values corresponding to reinforcement in the two mixes for this research are presented in Figures 4-5 as a function of exposure time. They are calculated from the polarization resistance values using a Stern-Geary constant of 26 mV. Corrosion current density is most widely treated as an indication of the corrosion performance of steel in concrete. Its values from  $0.1 \mu A/cm^2$  to  $0.5 \mu A/cm^2$  were used as the borderlines between passive and active corrosion as was indicated in previous work by Królikowski and Kuziak (2011).

Starting with values in the order of  $0.01 \mu A/cm^2$  corresponding to steel in passive condition according to earlier research by Pech-Canul and Castro (2002), there was tendency of  $I_{corr}$  to increase beyond  $0.2 \mu A/cm^2$  for  $MgCl_2$  contaminated sample, 4%  $Ca(NO_2)_2$  and 4%  $C_2H_7NO$  inhibited samples until 300 days exposure for 0.45 w/c ratios as evident in Figure-4. While 2% for all



three inhibitors, 4% *Bambusa arundinacea* and control sample were still within passive region for same exposure period. Also from Figure-5 only  $C_2H_7NO$  inhibitor and control sample were within passive region (that is, below  $0.2 \mu A/cm^2$ ) for the first 300 days of exposure before the other inhibitors reduced to within the passive region at 360 days exposure as a result of complete cement paste hydration. This behaviour is not surprising and is in agreement with earlier report by other authors (Jamil *et al.*, 2003; Dhouibi *et al.*, 2002; Tommaselli *et al.*, 2009; Pradhan, Bhattacharjee 2009).

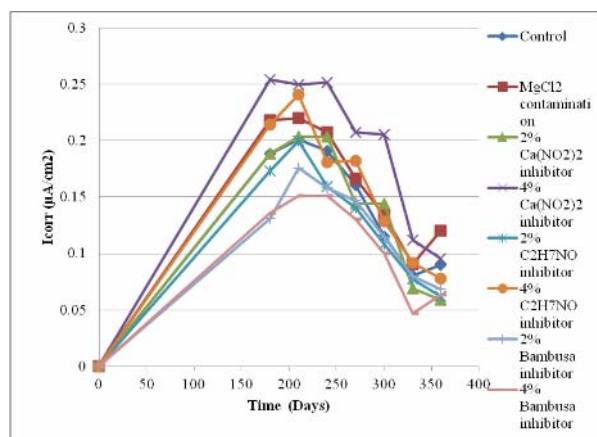


**Figure-4.** Corrosion current densities as functions of exposure time for a 0.45 w/c with 1.5%  $MgCl_2$  addition.

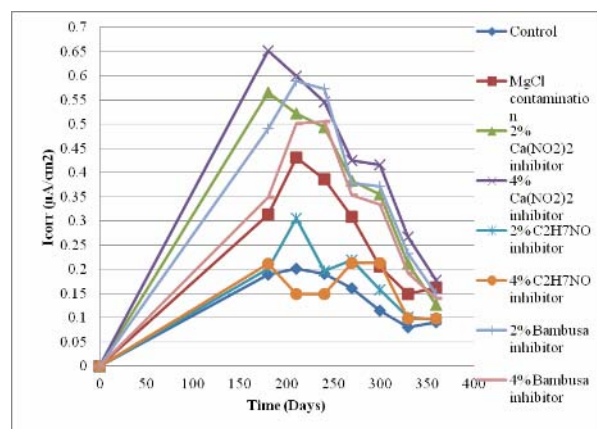


**Figure-5.** Corrosion current densities as functions of exposure time for a 0.45 w/c with 4.5%  $MgCl_2$  addition.

### 3.3. Electrochemical impedance spectroscopy (EIS) measurements

EIS is a powerful technique for obtaining detailed knowledge of conductive anode system and used to monitor electrical properties (material behaviour) of reinforced concrete in aggressive environment. It provides information on a number of parameters, such as the presence of surface films, interfacial reaction and mass-transfer phenomena (Jing, Wu, 2011). Impedance spectra (in Nyquist representation format) of EIS data obtained before and after the additions of the three inhibitors at the

different concentrations studied and used as corrosion inhibitors after 12 months of exposure in the corrosive medium (seawater) for wet and dry cycles are presented in Figures 6-9.

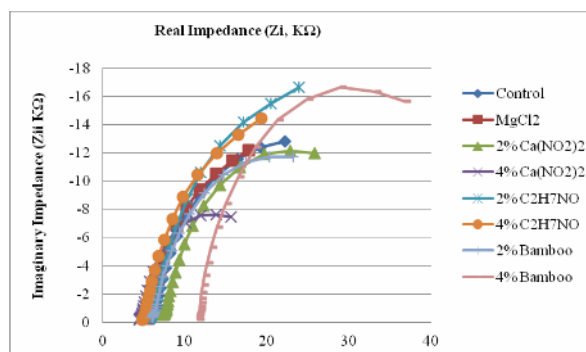


**Figure-6.** Nyquist impedance plot of rebar embedded in concrete for 0.45w/c with 1.5%  $MgCl_2$  contamination of 360 days exposure.

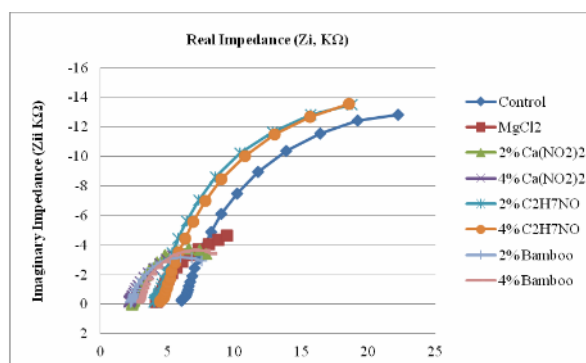


**Figure-7.** Nyquist impedance plot of rebar embedded in concrete for 0.45w/c with 4.5%  $MgCl_2$  contamination of 360 days exposure.

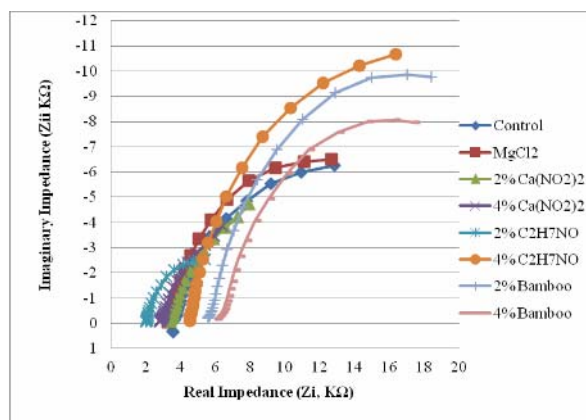


**Figure-8.** Nyquist impedance plot of rebar embedded in concrete for 0.65w/c with 1.5%  $MgCl_2$  contamination of 360 days exposure.



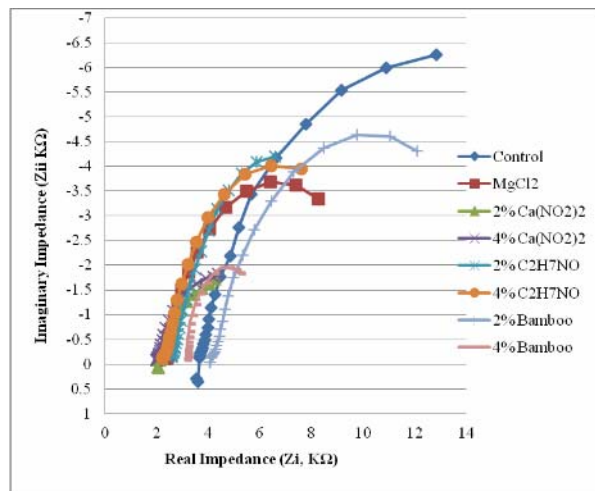


**Figure-9.** Nyquist impedance plot of rebar embedded in concrete for 0.65w/c with 4.5%  $\text{MgCl}_2$  contamination of 360 days exposure.

The results of EIS data shows that the concrete resistance ( $R_c$ ) and polarization resistance ( $R_p$ ) values were more higher for  $\text{Ca}(\text{NO}_2)_2$ ,  $\text{C}_2\text{H}_7\text{NO}$  and *Bambusa arundinacea* inhibitors admixture concrete as compared to the control and chloride contaminated concrete.  $R_c$  is considered to be high if the value is greater than 4 KΩ. But *Bambusa arundinacea* inhibitor was outstanding compared to two others inhibitors. This might be due to its pore blocking effects which prevented the formation of differential aeration of cells that promote corrosion on the steel surface as a result of oxygen level. Also the lower value of double layer capacitance  $C_{dl}$  of *Bambusa arundinacea* could be associated with its adsorption mode. This confirmed its adsorbed molecules paralleled to metal surface, and decreased the number of surface active sites due to its hydrophobic characteristics.

The non-linear reactive part of the electrode impedance contains double layer capacitance ( $C_{dl}$ ) and pseudo capacitance in the frequency measurement. In concrete, pseudo capacitance arises due to the adsorption of  $\text{OH}^-$ ,  $\text{K}^+$ ,  $\text{Na}^+$  and  $\text{Ca}^{2+}$  ions on the reinforcement surfaces. Vedalakshmi *et al.* (2009) suggested that if there is absence of double layer capacitance, then there will be no frequency dependence. But data presented in Figures 6-7 confirm that  $I_{corr}$  is dependent on frequency. Since the process may have large time constants, the reactive part of the impedance spectra cannot be eliminated completely. But at a lower frequency of 10 mHz, both passive and active conditions of reinforcement were fulfilled, ensuring that the measured current passes through the charge transfer resistance ( $R_p$ ) rather than  $C_{dl}$ . The double layer capacitance reduces after adsorption of the inhibitors since the adsorbed film reduces the dielectric constant between the metal and the cement paste electrolyte.

From Figures 6 and 8, the Nyquist plots shows the same pattern of trends for the *Bambusa arundinacea* inhibitor efficiency 360 days exposure for inhibition of  $\text{MgCl}_2$  contaminated concrete containing 0.94% chlorides,

even more than the control samples and other inhibitors. This might be attributed to the hydrophobic capacitive nature of the film ( $\gamma\text{-Fe}_2\text{O}_3$ ) formed on the rebar surface with a large time constant indicative of passive steel. The region of real impedance and imaginary impedance which increase continuously is known as Warburg impedance, which cause shielding or resistance effect for the metal corrosion according to similar research by Ali *et al.* (2007). The observed impedance of the inhibitors is as a result of the slow diffusion of oxygen through the concrete matrix and the dielectric film component of solid hydroxide layer at the steel-concrete interface. These processes can be attributed to the electrochemical reaction on the electrode (film) surface and the associated charge-transfer resistance and double-layer capacitance which was also observed in previous work by Tommaselli *et al.* (2009).

On the other hand, in the contaminated concrete containing 2.82% chloride, the Nyquist plot yields a shorten curve indicating the break-down of dielectric film due to chlorides which can be observed in Figures 7 and 9. The addition of chloride decreases the charge transfer resistance which indicates the competition between the aggressive chloride ions and the passivating hydroxyl ions. Chloride ion might have reacted with hydrated tricalciumaluminate ( $\text{C}_3\text{A}$ ) hydrate to form chloroaluminate ( $\text{C}_3\text{A} \cdot \text{CaCl}_2 \cdot 10\text{H}_2\text{O}$ ) which may contain 75-90% chloride according to study by Indrajit *et al.* (2011). Since it has exceeded threshold chloride level, the protective passive layer would be destroyed as in the case of chloride contaminated samples. In general, the chloride threshold is taken to be 0.15% of the soluble chloride by weight of cement. So, 0.94% and 2.82% chloride has far exceeded the commonly accepted corrosion threshold in this work.

It is important to note that the three inhibitors exhibited almost the same behaviour during all the test times and for all the concentrations. The polarization resistance ( $R_p$ ) of the steel surface representing the resistance to current flow across the steel-concrete interface at a corrosion potential, is dependent on the formation of passive film of iron hydroxides/oxides during the process of corrosion and is expected to decrease if this protective film is broken under certain conditions.  $R_p$  which is the rate determining resistance at the reinforcing steel corrosion, therefore, as the  $R_p$  increases the corrosion rate decreases and the capacitance of interface also decreases. This is evident in this work as inhibited contaminated concrete shows low corrosion rate. But *Bambusa arundinacea* exhibited lowest corrosion rate,  $C_{dl}$  and highest  $R_p$  values for the entire period of exposure. The large arcs observed from high to low frequencies in Figures 6-9, indicates that the polarization resistance,  $R_p$ , becomes dominant due to adsorption of inhibitors. Also the inhibition efficiency derived from the  $R_p$  values of the impedance measurement shows that *Bambusa arundinacea* is consistently higher compared to other two inhibitors for 0.45w/c at 1.5%  $\text{MgCl}_2$  contamination. Only ethanolamine inhibition efficiency was adequate for



0.45w/c at high 4.5%  $\text{MgCl}_2$  contamination. Inhibition efficiency was derived from the below expression according to Cruz *et al.* (2004).

$$\%IE (R_p) = \frac{R_p(\text{inh}) - R_p}{R_p(\text{inh})} \times 100,$$

Where  $R_p$  is the polarization resistance without inhibitor and  $R_p(\text{inh})$  is the polarization resistance with inhibitor. Meanwhile the  $R_p$  values obtained from impedance measurements enable us to validate corrosion inhibition properties of these three inhibitors studied as a function of time.

#### 4. CONCLUSIONS

In view of the outlined objectives earlier mentioned in this research work and subsequent series of investigations conducted as well as the results obtained, the following conclusions were drawn:

- The electrode potentials of reinforcing steel were not indicative of early corrosion likelihood in the concrete mix.
- The potential results of all the inhibitors and their inhibitions were adequate for 0.45 w/c ratios, but *Bambusa arundinacea* standout for excellent inhibition.
- Corrosion current density ( $I_{\text{corr}}$ ) which represents instantaneous rate of corrosion at the particular time of voltage measurement, increases beyond  $0.2 \mu\text{A}/\text{cm}^2$  for  $\text{MgCl}_2$  contaminated sample, 4%  $\text{Ca}(\text{NO}_3)_2$  and 4%  $\text{C}_2\text{H}_7\text{NO}$  inhibited samples at age of 360 days exposure for 0.45 w/c ratios. While 2% for all three inhibitors, 4% *Bambusa arundinacea* and control sample were still within passive region for same exposure period.
- The pore blocking effects of *Bambusa arundinacea* prevented the formation of differential aeration of cells that promote corrosion on the steel surface as a result of oxygen level due to its high concrete resistance. Also, the lower value of double layer capacitance  $C_{\text{dl}}$  of *Bambusa arundinacea* could be associated with its adsorption mode. This confirmed its adsorbed molecules paralleled to metal surface, and decreased the number of surface active sites due to its hydrophobic characteristics. The double layer capacitance reduces after adsorption of the inhibitors since the adsorbed film reduces the dielectric constant between the metal and the cement paste electrolyte.
- The addition of chloride decreases the polarization resistance ( $R_p$ ) which indicates the competition between the aggressive chloride ions and the passivating hydroxyl ions. *Bambusa arundinacea* exhibited lowest corrosion rate, lowest  $C_{\text{dl}}$  and highest  $R_p$  values for the entire period of exposure despite exceeding chloride threshold value.
- Nyquist plots shows the same pattern of trends for the *Bambusa arundinacea* inhibitor efficiency at 360 days exposure for inhibition of  $\text{MgCl}_2$  contaminated

concrete containing 0.94% chlorides, even more than the control samples and other inhibitors. This might be attributed to the hydrophobic capacitive nature of the film ( $\gamma\text{-Fe}_2\text{O}_3$ ) formed on the rebar surface with a large time constant indicative of passive steel, the region of real impedance and imaginary impedance which increase continuously cause shielding or resistance effect for the metal corrosion. The observed impedance of this inhibitor is as a result of the slow diffusion of oxygen through the concrete matrix and the dielectric film component of solid hydroxide layer at the steel-concrete interface.

- It was observed that corrosion rate is inversely proportional to concrete resistance. Thus resistance can be considered as general parameter for describing performance of reinforced concrete structures subjected to chloride contamination.

#### ACKNOWLEDGEMENTS

This work was financially supported by Federal University of Technology Minna, Nigeria and Construction Research Alliance, Universiti Teknologi Malaysia (UTM), Johor Bahru, Johor Malaysia.

#### REFERENCES

- Abdulahman A.S. and Ismail M. 2012. Evaluation of corrosion inhibiting admixtures for steel reinforcement in Concrete. International Journal of the Physical Sciences. 7(1): 139-143.
- Abdulahman A.S., Ismail M. and Hussain M.S. 2011a. Corrosion inhibitors for steel reinforcement in concrete: A review. Scientific Research and Essays. 6(20): 4152-4162.
- Abdulahman A.S., Ismail M. and Hussain M.S. 2011b. Inhibition of Corrosion of Mild Steel in Hydrochloric Acid by *Bambusa Arundinacea*. International Review of Mechanical Engineering. 5(1): 59-63.
- Ali G.A., Kayakırlmaz K. and Erbil M. 2007. The effect of thiosemicarbazide on corrosion resistance of steel reinforcement in concrete. Construction and Building Materials. 21: 669-676.
- Ann K.Y., Jung H.S., Kim H.S., Kim S.S. and Moon H.Y. 2006. Effect of Calcium nitrite-based corrosion inhibitor in preventing corrosion of embedded steel in concrete. Cement Concrete Research. 36: 530-535.
- Boltryk M., Pawluczuk E. and Ratkowska W. 2011. Influence of Asphalt addition and consolidation method on durability of cement concrete. Journal of Civil Engineering and Management. 17(4): 476-482.
- Cruz J.R., Martinez J.D. and García-Ochoa E. 2004. Experimental and theoretical study of 1-(2-ethylamino)-2-methylimidazole as an inhibitor of carbon steel corrosion



- in acid media. *Journal of Electroanalytical Chemistry*. 566(1): 111-121.
- De-Schutter G. and Luo L. 2004. Effect of corrosion inhibiting admixtures on concrete properties. *Construction and Building Materials*. 18(7): 483-489.
- Dhouibi L., Triki E. and Raharinaivo A. 2002. The application of electrochemical impedance spectroscopy to determine the long-term effectiveness of corrosion inhibitors. *Cement and Concrete Composites*. 24: 35-43.
- Indrajit R., George C.P. and Julio F.D. 2011. Effect of Concrete Substrate Repair Methods for Beams Aged by Accelerated Corrosion and Strengthened with CFRP. *Journal of Aerospace Engineering*. pp. 227-239.
- Ismail M., Abdulrahman A.S. and Hussain M.S. 2011. Solid Waste as Environmental Benign Corrosion Inhibitors in Acid Medium. *International Journal of Engineering Science and Technology (IJEST)*. 3(2): 1742-1748.
- Ismail M., Muhammad B. and Ismail M. E. 2010a. Compressive strength loss and reinforcement degradations of reinforced concrete structure due to long-term exposure. *Construction and Building Materials*. 24(6): 898-902.
- Ismail M., Hamza E., Goh C.G. and Ihsan A. 2010b. Corrosion performance of dual-phase steel embedded in concrete. *The Arabian Journal for Science and Engineering*. 35(2B): 81-90.
- Jamil H.E., Montemor M.F., Boulif R., Shrirri A. and Ferreira M.G.S. 2003. An electrochemical and analytical approach to the inhibition mechanism of an amino-alcohol-based corrosion inhibitor for reinforced concrete. *Electrochimica Acta*. 48(23): 3509-3518.
- Jing X. and Wu Y. 2011. Electrochemical studies on the performance of conductive overlay material in cathodic protection of reinforced concrete. *Construction and Building Materials*. 25: 2655-2662.
- Kondratova I. L., Montes P. and Bremner T.W. 2003. Natural marine exposure results for reinforced concrete slabs with corrosion inhibitors. *Cement and Concrete Composites*. 25(4-5): 483-490.
- Królikowski A. and Kuziak J. 2011. Impedance study on calcium nitrite as a penetrating corrosion inhibitor for steel in concrete. *Electrochimica Acta*. 56(23): 7845-7853.
- Pech-Canul M.A. and Castro P. 2002. Corrosion measurements of steel reinforcement in concrete exposed to a tropical marine atmosphere. *Cement and Concrete Research*. 32: 491-498.
- Pradhan B. and Bhattacharjee B. 2009. Performance evaluation of rebar in chloride contaminated concrete by corrosion rate. *Construction and Building Materials*. 23(6): 2346-2356.
- Raafat E.H., Mirman A., Cook A. and Rizkalla S. 2011. Effectiveness of Surface- Applied Corrosion Inhibitors for Concrete Bridges. *Journal of Materials In Civil Engineering*. pp. 271-280.
- Raja P.B. and Sethuraman M.G. 2008. Natural products as corrosion inhibitor for metals in corrosive media - A review. *Materials Letters*. 62(1): 113-116.
- Rwamamara R. and Simonson P. 2012. Self-compacting concrete use for construction work environment sustainability. *Journal of Civil Engineering and Management*. 18(5): 724-734.
- Tommaselli M.A.G., Mariano N.A. and Kuri S.E. 2009. Effectiveness of corrosion inhibitors in saturated calcium hydroxide solutions acidified by acid rain components. *Construction and Building Materials*. 23: 328-333.
- Uhlig H.H. 2004 *Corrosion and Corrosion Control*, George Harrap and Co. Ltd.
- Vedalakshmi R., Manoharan S.P., Song H.W. and Palaniswamy N. 2009. Application of harmonic analysis in measuring the corrosion rate of rebar in concrete. *Corrosion Science*. 51: 2777-2789.
- Vishnudevan M. and Thangavel K. 2006. Evaluation of organic based corrosion inhibiting admixtures for reinforced concrete. *Anti-Corrosion Methods and Materials*. 53(5): 271-276.